

Received: 2017.10.13
Accepted: 2017.11.15
Published: 2017.12.06

Investigations of Cartilage Matrix Degeneration in Patients with Early-Stage Femoral Head Necrosis

Authors' Contribution:
Study Design A
Data Collection B
Statistical Analysis C
Data Interpretation D
Manuscript Preparation E
Literature Search F
Funds Collection G

ABCE 1,2 Ronghua Xu*
ABCE 1,3,4 Bo Wei*
DEF 1,3,4 Jiayi Li
CDF 1,4 Chenyu Huang
CDF 1,4 Rongcai Lin
DEF 1,3,4 Cheng Tang
DEF 1,3,4 Yan Xu
DEF 1,3,4 Qingqiang Yao
ABCDEF 1,3,4 Liming Wang

1 Department of Orthopedics, Nanjing First Hospital, Nanjing Medical University, Nanjing, Jiangsu, P.R. China
2 Department of Orthopedics, The Affiliated Xuzhou Hospital of Medical College of Southeast University, Xuzhou, Jiangsu, P.R. China
3 Cartilage Regeneration Center, Nanjing First Hospital, Nanjing Medical University, Nanjing, Jiangsu, P.R. China
4 Digital Medicine Institute, Nanjing Medical University, Nanjing, Jiangsu, P.R. China

* These authors contributed equally to this study and share first authorship

Corresponding Author: Liming Wang, e-mail: limingwang99@hotmail.com

Source of support: This research was sponsored by the National Natural Science Foundation of China (Grant No. 81702148), the Natural Science Foundation of Jiangsu Province of China (Grant No. BK20170139), and the Orthopedic Clinical Medical Center of Nanjing City of China

Background: The purpose of this study was to explore changes in cartilage matrix in early-stage femoral head necrosis (FHN).


Material/Methods: Femoral head samples of patients with early FHN were collected during total hip arthroplasty (THA), high-field 7.0T MRI scans were performed *in vitro*, and the average T2 values were calculated. Cartilage samples were obtained from the weight-bearing area (FHN group) and non-weight-bearing area (Control group), divided into 3 equal parts and used for biochemical analysis, histopathological staining, and gene expression analysis.

Results: T2 mapping of the femoral head specimens showed that the density distribution of cartilage surface was not uniform, and the average T2 value increased unevenly. Histological staining demonstrated that the number of chondrocytes was significantly decreased and they were irregularly arranged, SO staining was lost, and collagen fiber arrangement was slightly more irregular on the cartilage surface in the FHN group. The biochemical results in the FHN group showed that the water content increased significantly and the DNA content decreased significantly, while no significant changes in GAG and total collagen contents were detected. Gene expression analysis in the FHN group showed that SOX9 expression was significantly down-regulated, while COL10A1 and RUNX2 expressions were significantly up-regulated. The expression of ACAN and COL2A1 were decreased and COL1A1 was increased, but there was no significant difference compared with the Control group.

Conclusions: Taken together, the results of this study suggest that patients with early-stage FHN tend to have cartilage matrix degeneration, which provides new ideas for studying the pathogenesis of FHN and selecting treatment strategies.

MeSH Keywords: **Femur Head Necrosis • Macular Degeneration • Magnetic Resonance Imaging • Matrilin Proteins**

Full-text PDF: <https://www.medscimonit.com/abstract/index/idArt/907522>

 3210

 1

 5

 37



Background

Femoral head necrosis (FHN) is a common clinical disease in orthopedics, and about 2–3 million patients are diagnosed with FHN every year in the United States [1]. The pathological morphology of FHN shows femoral head collapse deformation, trabecular bone discontinuity, and subchondral bone structure damage; trabecular bone in the sclerosis area is proliferated, the number is increased, the arrangement is compact, and a variety of hyperplasia tissues are formed [2]. The specific pathogenesis of FHN and the factors that affect the progression of the disease are not yet fully understood. However, patient clinical manifestations and imaging findings (such as the collapse of the femoral head) help to assess the extent of FHN [3,4]. After collapse of the femoral head, most patients need to undergo total hip arthroplasty (THA) [5]. Young patients with a relatively long life expectancy and higher activity may require revision surgery at some time after THA. Therefore, some treatment methods in FHN patients before femoral head collapse may be beneficial to delay THA surgery. The current early treatment options include drug therapy, extracorporeal shock wave therapy, core decompression, tantalum rod implantation, bone grafts (without vascular pedicle), and stem cell transplantation therapy [6–11]. The various treatment options each have their advantages, but there are shortcomings, such as the high failure rate of treatment and lack of long-term follow-up results [12]. Therefore, early diagnosis of FHN is critical in the selection of treatment methods and the prognosis of the disease.

At present, FHN has a variety of diagnostic methods, of which hip anteroposterior and frog radiographs can be used for screening FHN in the early stage of the disease. CT scanning is less sensitive than MRI and increases the risk of radiation-associated damage; MRI detection is a diagnosis and treatment technology for early FHN, with high sensitivity and specificity [13,14]. With the rapid development of high-field MRI technology, researchers can more accurately detect the abnormal changes of bone microstructure and articular cartilage in the femoral head of patients [15]. Theysohn et al. used high-field 7.0T MRI to scan the hip joints of patients with FHN, and found that it can better demonstrate anatomical and pathological changes [16]. Further, Theysohn et al. compared the image evaluation of 7.0T and 3.0T MRI in patients with FHN, and found that they have a similar effect on hip joint imaging, but 7.0T MRI has more advantages in image contrast (e.g., it can more accurately display the cartilage defect changes) and detection of liquid [17]. In our previous study, we used high-field 7.0T MRI to examine femoral head samples and found that it accurately detected early degenerative changes in the femoral head cartilage [18].

Based on current understanding of the pathogenesis of FHN, it is generally considered to be a type of bone disease. After femoral head collapse, structural damage to the subchondral bone causes changes in mechanical stimulation (stress environment), which then causes degeneration of articular cartilage [19]. Ruch et al. observed the cartilage surface using hip arthroscopy in patients with FHN, and found that there are many osteochondral degenerations that cannot be detected by X-ray and MRI scanning [20]. Magnussen et al. reported that the histological changes and mechanical strength of post-collapse articular cartilage have a high correlation with the gross morphology of articular cartilage surface in patients with FHN, and further demonstrated changes in mechanical characteristics (tensile, compressive, and shear forces) caused by femoral head necrosis [21,22]. However, these studies focused on late-stage FHN after collapse of the femoral head, and there are few studies on the early stage of FHN prior to collapse. In addition, previous studies have focused on changes in gross appearance and mechanical properties of articular cartilage caused by necrosis of the femoral head, and there is no published study on changes in the articular cartilage matrix induced by FHN. Therefore, it is of great importance to explore changes in the articular cartilage matrix associated with early necrosis of the femoral head, which is crucial for the selection of treatment strategies and prevention of the disease.

Therefore, we propose the scientific hypothesis that early-stage femoral head necrosis is accompanied by degeneration of the articular cartilage matrix, which provides new ideas for studying the pathogenesis of FHN and selecting treatment strategies. In the present study, we collected femoral head samples from patients with early-stage FHN and used gross observation, high-field 7.0T MRI scans, histological staining, cartilage biochemical analysis, and gene expression detection performed *in vitro* to test this hypothesis.

Material and Methods

Patient selection and collection of femoral head samples

The patients in this study were selected from among patients with unilateral idiopathic FHN who underwent THA from May 2014 to August 2016 at Nanjing First Hospital affiliated to Nanjing Medical University (Figure 1A). According to Ficat staging [23], we selected 10 patients (6 males and 4 females) with stage II disease, with a mean age of 60.8 years (55–66 years). Femoral head samples were collected during the THA operation (Figure 1B) and stored in a deep cryogenic freezer at –80°C. The experimental protocol of this study was approved by the Ethics Committee of Nanjing Medical University, and written informed consent was obtained from all participants.

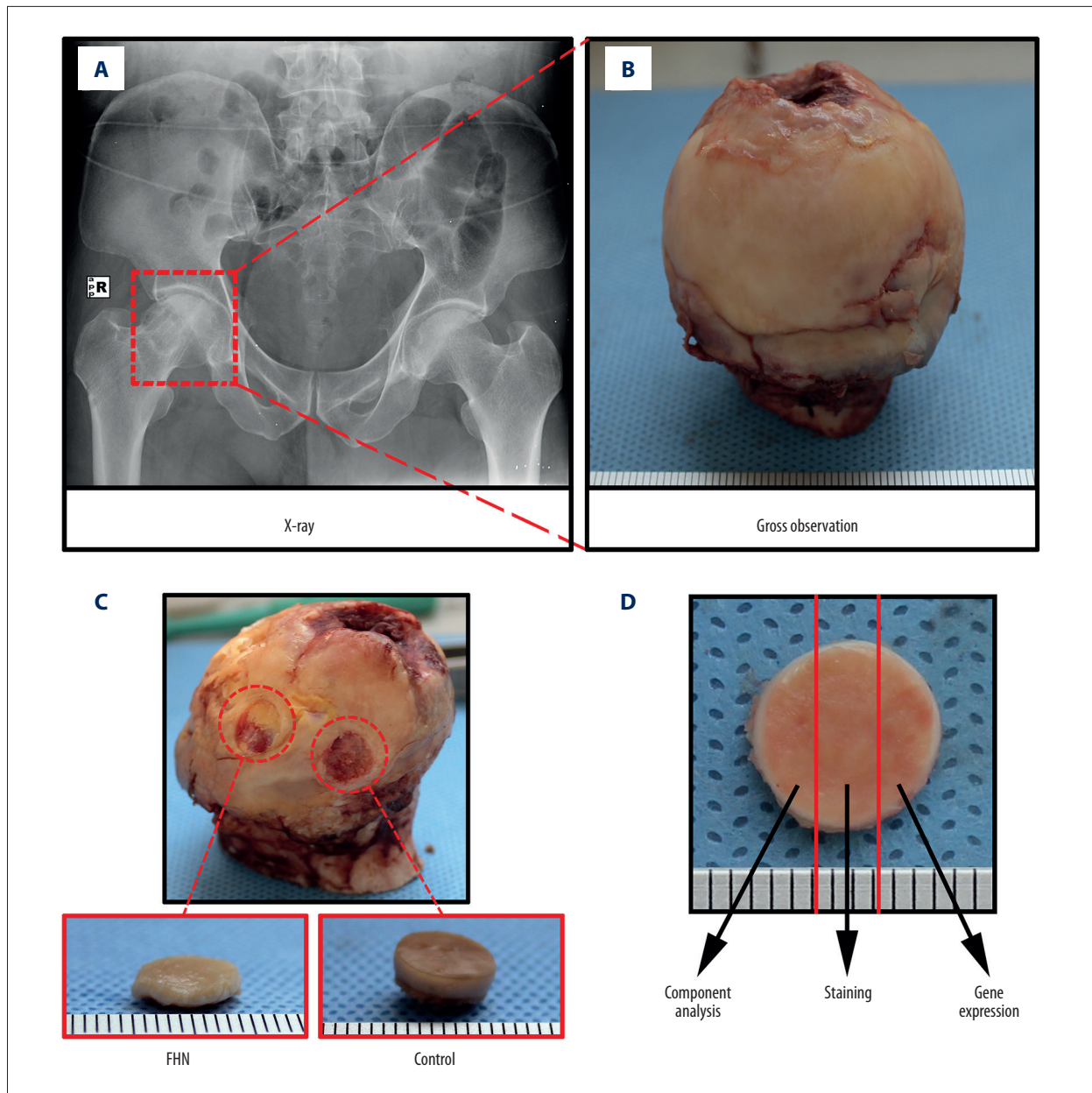


Figure 1. Patient selection, collection, and segmentation of femoral head samples. **(A)** The patients were selected from among patients with unilateral noninvasive FHN who underwent THA. **(B)** Femoral head samples were collected during the THA operation. **(C)** Osteochondral samples with a diameter of 8 mm were obtained from the weight-bearing and non-weight-bearing areas of the femoral head as the femoral head necrosis group (FHN group) and the control group (Control group), respectively. **(D)** Cartilage samples were divided into 3 equal parts and used for biochemical analysis, histopathological staining, and gene expression analysis.

7.0T MRI detection

We used the 7.0T MRI Bruker system (PharmaScan Bruker, BioSpin Karlsruhe, Germany) equipped with a 60-mm coil to examine the femoral head samples. The following parameters were used for the sagittal T2 mapping scan: repetition time (TR) 3800 milliseconds, echo time (TE) 36 milliseconds, flip angle

(FA) 180 degrees, field of view (FOV) 60×60 mm, pixel matrix 384×384, section thickness 1.2 mm, scanning time of 21 minutes 16 seconds 800 milliseconds. Next, the T2 map was generated using the Bruker ParaVision 5 system. Four different regions of interest were selected from the cartilage surface of each femoral head. The average T2 relaxation time was calculated using the Bruker ParaVision 5 system, and the regions

of interest were analyzed by an experienced radiologist with 6 years of experience with musculoskeletal disorders.

Sample selection and segmentation

After MRI examination, the round osteochondral samples with a diameter of 8 mm were obtained using a biological punch from the weight-bearing area and non-weight-bearing area of the femoral head as the femoral head necrosis group (FHN group) and the control group (Control group), respectively (Figure 1C). After gross observation, the cartilage samples were divided into 3 equal parts using a surgical blade, and then were used for biochemical analysis, histopathological staining, and gene expression analysis (Figure 1D).

Histological staining

Samples for histological staining were fixed in 10% neutral formaldehyde solution at room temperature for 24 h, decalcified with 5% nitric acid for 48 h, and rinsed well with running water for 12 h. After gradient alcohol dehydrated tissue and the transparent tissue of toluene, it was immersed in pre-melted paraffin and kept at 65°C overnight. The next day, the tissues were embedded in paraffin blocks and cut into sections with uniform thickness of 5 µm. Then, the morphology and distribution of chondrocytes were detected by hematoxylin-eosin (HE) staining, the distribution of proteoglycan was examined by Safranin O-fast green (SO) staining, and the arrangement of collagen fibers was observed by Sirius red staining. The staining results were observed using an inverted fluorescence microscope (Ci-L; Nikon, Tokyo, Japan).

Biochemical component analysis

The cartilage samples for biochemical composition analysis were weighed to obtain their wet weights, dried at 65°C for 2 days to remove the moisture, and weighed to obtain dry weights. The water content of the cartilage samples was calculated as: wet weight–dry weight/wet weight. The DNA content of the cartilage samples was examined using the Qubit dsDNA kit (Invitrogen, Eugene, OR, USA). First, the cartilage samples were digested with papain, and the digested solution was reacted with the Hoechst 33258 staining solution in the dark for 30 min. Fluorescence intensity was detected using a microplate reader (Bio-Rad Laboratories, Richmond, CA, USA) at an excitation wavelength of 360 nm and an emission wavelength of 460 nm. The glycosaminoglycan (GAG) content of the cartilage samples was examined using a Blyscan (TM) sulfated GAG assay kit (Bicolor, Newton Abbey, UK). First, papain-digested cartilage samples were mixed with Blyscan staining and centrifuged at 12 000 rpm for 10 min. After removing the unbound GAG dye solution, the separation reagent was added to the remaining granular material at the bottom

Table 1. Detailed information about the primer sequences used for RT-PCR.

Gene	Primer nucleotide sequence
SOX9	Forward: 5-TTCCGCGACGTGGACAT-3
	Reverse: 3-TCAAACCTCGTTGACATCGAAGGT-5
Agreecan (ACAN)	Forward: 50-TCGAGGACAGCGAGGCC-3
	Reverse: 3-TCGAGGGTGTAGCGGTAGAGA-5
Type II collagen (COL2A1)	Forward: 5-GGCAATAGCAGGTTCCAGTACA-3
	Reverse: 3-CGATAACAGTCTTGCCCCACTT-5
Type I collagen (COL1A1)	Forward: 5-CAGCCGCTTCCACTACAGC-3
	Reverse: 3-TTTTGTATTCAATCACTGTCTTGCC-5
Type X collagen (COL10A1)	Forward: 5-CAAGGCACCATCTCCAGGAA-3
	Reverse: 3-AAAGGGTATTGTGGCAGCATATT-5
RUNX2	Forward: 5-GGAGTGGACGAGGCAAGAGTTT-3
	Reverse: 3-AGCTTCTGTCTGTGCTTCTGG-5
GAPDH	Forward: 5-ATGGGGAAGGTGAAGTTCG-3
	Reverse: 3-TAAAAGCAGCCCTGGTGACC-5

of the tube. The absorbance was measured at a wavelength of 656 nm using a microplate reader. Total collagen content of the cartilage samples was assayed using the Sircol Collagen Assay kit (Bicolor, Newton Abbey, UK). The pepsin-digested cartilage samples were mixed with the Sircol dye and centrifuged at 12 000 rpm for 10 min. After removing the supernatant, the granular precipitate at the bottom of the tube was washed with an acid salt cleaning agent and dissolved in an alkaline reagent. The absorbance was measured at 555 nm using a microplate reader.

Gene expression detection

Cartilage samples for gene expression detection were washed 3 times with PBS, pre-chilled Trizol reagent (Invitrogen, USA) was added and milled in a tissue homogenizer, and RNA was further isolated and stored at –80°C. The optical density (OD) of the sample was determined to be 260 nm and 280 nm. OD260/280 was found to be highly purified extracted RNA at 1.8–2.1. Further, SOX9, proteoglycans (ACAN), type II collagen (COL2A1), type I collagen (COL1A1), type X collagen (COL10A1), Runt-related transcription factor 2 (RUNX2), and glyceraldehyde- 3-phosphate dehydrogenase (GAPDH) gene expression of cartilage samples were detected using a Real-Time PCR instrument (Applied Biosystems, USA) and Real-Time PCR Master Mix (SYBR Green) kit (TOYOBO, Japan). Each sample was tested 3 times. The primer sequences of the genes are shown in Table 1.

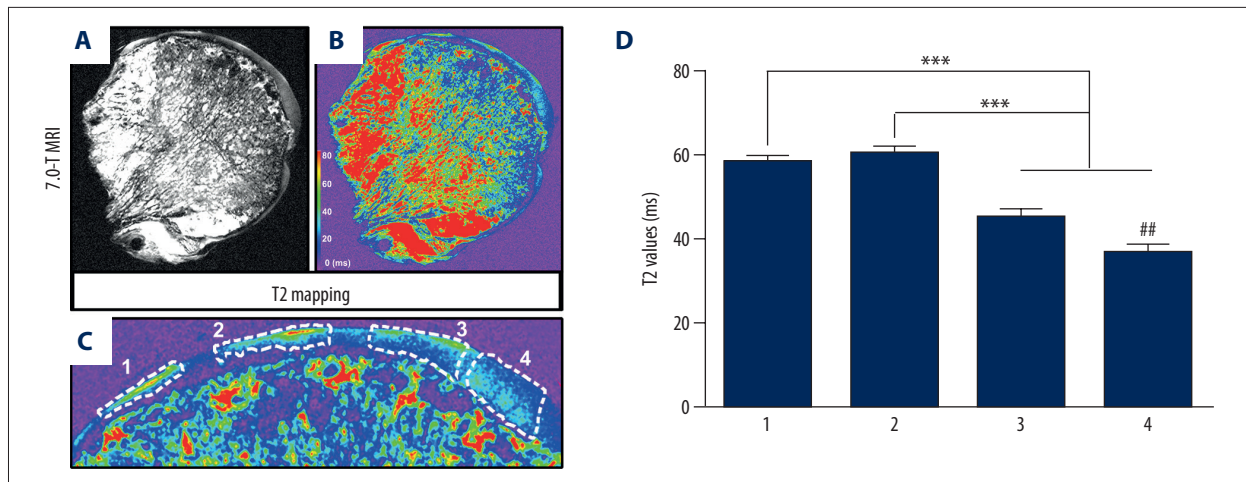


Figure 2. 7.0T MRI T2 mapping and T2 value analysis of femoral head cartilage. (A) We found disorganization of the trabecular bone structure, uneven density distribution, and poor continuity with the surface cartilage. (B) The signal intensity of cartilage surface increased unevenly, and the signal intensity of subchondral bone was increased or interrupted. (C) Four different regions of the cartilage surface from the femoral head were selected as regions of interest, and the average T2 relaxation time was calculated. (D) The average T2 value of the femoral head cartilage surface was unevenly increased.

Statistical analysis

The univariate analysis of variance (ANOVA) and LSD methods were used to compare the differences in T2 values among the 4 regions of interest selected from the cartilage surface of the FHN specimen. The non-paired *t* test was used to compare the differences in biochemical components (water, DNA, GAG, and total collagen content) and gene expression (SOX9, ACAN, COL2A1, COL1A1, COL10A1, and RUNX2) between the FHN group and the Control group, respectively. $P < 0.05$ was considered to be statistically significant. All data are expressed as mean \pm standard deviation (SD). All statistical analyses were performed using SPSS 13.0 statistical software (SPSS, Chicago, USA).

Results

7.0T MRI T2 mapping and T2 value analysis of femoral head cartilage

The T2 mapping of the femoral head specimens showed disorganization of the trabecular bone structure, uneven density distribution, poor continuity with the surface cartilage, and uneven density distribution of the articular cartilage surface (Figure 2A). T2 mapping pictures showed that the signal intensity of cartilage surface increased unevenly, and the signal intensity of subchondral bone appeared increased or interrupted (Figure 2B). In addition, 4 different regions of the cartilage surface from the femoral head were selected as regions of interest, and the average T2 relaxation time was calculated (Figure 2C). The results showed that the average T2 value of

region 1 and region 2 were significantly higher than that of region 3 and region 4 ($P < 0.001$), and the average T2 value of region 3 was significantly higher than that of region 4 ($P < 0.01$), but no significant difference in the average T2 value between region 1 and region 2 was detected ($P > 0.05$) (Figure 2D), indicating that the average T2 value of the femoral head cartilage surface was unevenly increased, which suggests the possibility of cartilage degeneration.

Histological staining of femoral head cartilage

HE staining of femoral head samples showed that the number of chondrocytes on the cartilage surface of the FHN group was significantly decreased and the cell arrangement was irregular (Figure 3A), while the number and arrangement of chondrocytes were relatively normal in the Control group (Figure 3B). SO staining of the femoral head specimens showed uneven deposition of cartilage GAG in the FHN group, and there was a significant loss of SO staining on the cartilage surface (Figure 3C). However, the Control group showed uniform distribution of SO staining throughout the cartilage layer (Figure 3D). Sirius red staining of the femoral head specimens showed that the collagen fibers of the FHN group were slightly irregular in the surface layers and normal in the lower layers (Figure 3E), while the collagen fibers were well-arranged in the Control group (Figure 3F).

Biochemical composition analysis of femoral head cartilage

Water content in the FHN group was significantly higher than that in the Control group ($P < 0.05$; Figure 4A), and DNA content

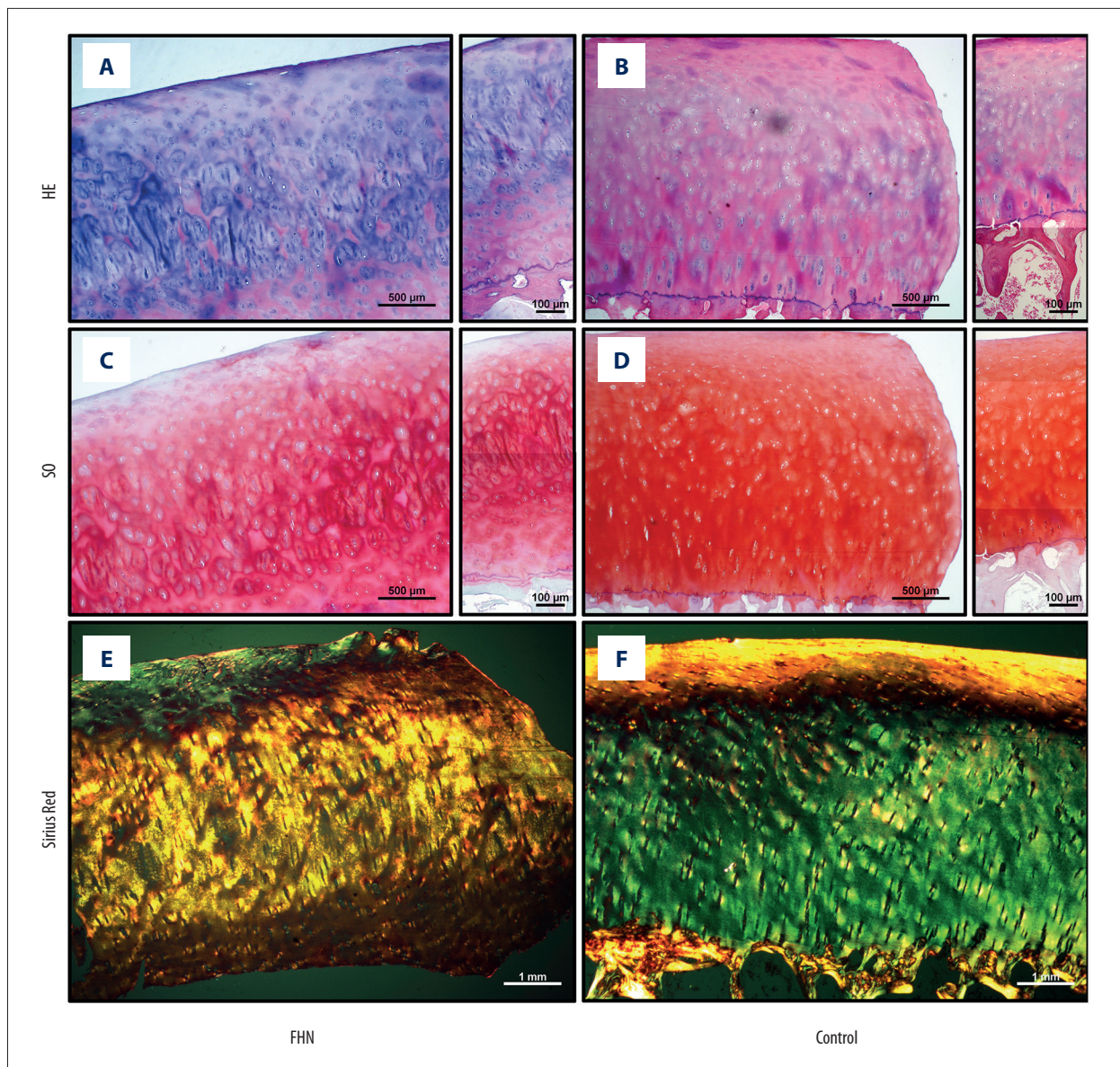


Figure 3. Histological staining of femoral head cartilage. (A) The number of chondrocytes on the cartilage surface of the FHN group was significantly decreased and the cell arrangement was irregular. (B) The number and arrangement of chondrocytes were relatively normal in the Control group. (C) There was a significant loss of SO staining on the cartilage surface. (D) The Control group showed uniform distribution of SO staining throughout the cartilage layer. (E) The collagen fibers of the FHN group were slightly irregular in the surface layers and were normal in the lower layers. (F) The collagen fibers were well-arranged in the Control group.

in the FHN group was significantly lower than that in the Control group ($P < 0.01$; Figure 4B). The content of GAG in the FHN group was slightly lower than that in the Control group, and the total collagen content in the FHN group was slightly higher than that in the Control group, but there was no detectable significant difference ($P > 0.05$; Figure 4C).

Gene expression detection of femoral head cartilage

The expression of SOX9 gene in the FHN group was significantly lower than that in the Control group ($P < 0.01$; Figure 5A). The expressions of ACAN and COL2A1 gene in the FHN group were lower than those in the Control group, and the expression of COL1A1 gene in the FHN group was higher than that in the Control group, but the differences were not statistically significant ($P > 0.05$; Figure 5B–5D). Moreover, the expression of

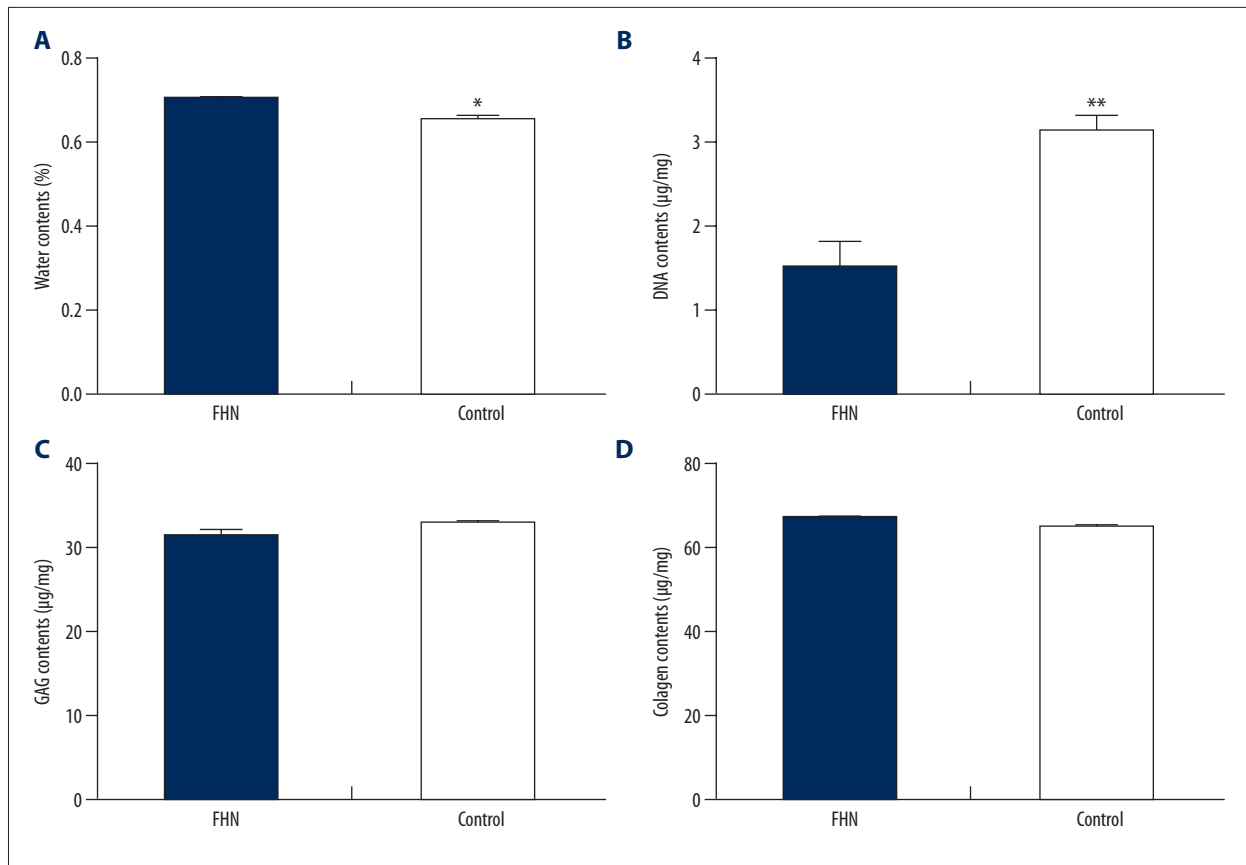


Figure 4. Biochemical composition analysis of femoral head cartilage. (A) Water content in the FHN group was significantly higher than that in the Control group. (B) DNA content in the FHN group was significantly lower than that in the Control group. (C, D) The content of GAG in the FHN group was slightly lower than that in the Control group, and the total collagen content in the FHN group was slightly higher than that in the Control group, but there was no detectable significant difference ($P>0.05$).

COL10A1 and RUNX2 gene in the FHN group was significantly higher than that in the Control group ($P < 0.05$; Figure 5E, 5F).

Discussion

In this study, we used the high-field 7.0T MRI and T2 mapping technique to accurately detect the abnormal cartilage changes of femoral head specimens in patients with early-stage FHN. T2 mapping of the femoral head samples showed that the density distribution of articular cartilage surface was not uniform, and the average T2 value of the femoral head cartilage surface increased unevenly, suggesting early cartilage degeneration. The normal articular cartilage matrix consists of water, GAG, and type II collagen. The cartilage matrix surrounding chondrocytes plays an important role in maintaining the biomechanical properties of articular cartilage. In the early stages of cartilage degeneration, the cartilage undergoes degradation of the matrix network structure, including increased water content, decreased GAG content, and disordered collagen fiber structure; the reduction in GAG content

further causes increase in water content and disordered collagen fiber structure [24, 25]. MRI has significant advantages in assessing late-stage articular cartilage degeneration and soft tissue abnormalities. However, it is difficult to accurately detect cartilage matrix changes associated with early cartilage degeneration using conventional MRI techniques [26]. With the development of high-field MRI and quantitative MRI technology, researchers can more accurately evaluate changes in the cartilage matrix [27,28]. Among these, T2 mapping is an effective technique for detecting early cartilage degeneration, especially monitoring changes in water content and collagen network structure, which has been confirmed in many *in vitro* and *in vivo* experimental studies [29–31]. Apprigh et al. found that the water content of articular cartilage decreased with increased joint stress [32], and it has been reported that increased cartilage T2 relaxation time is accompanied by disruption of the matrix structure, especially the increased water content and loss of collagen integrity [33]. Thus, articular cartilage stress and decreased GAG content result in increased water content and fluidity, leading to an increase in the T2 value.

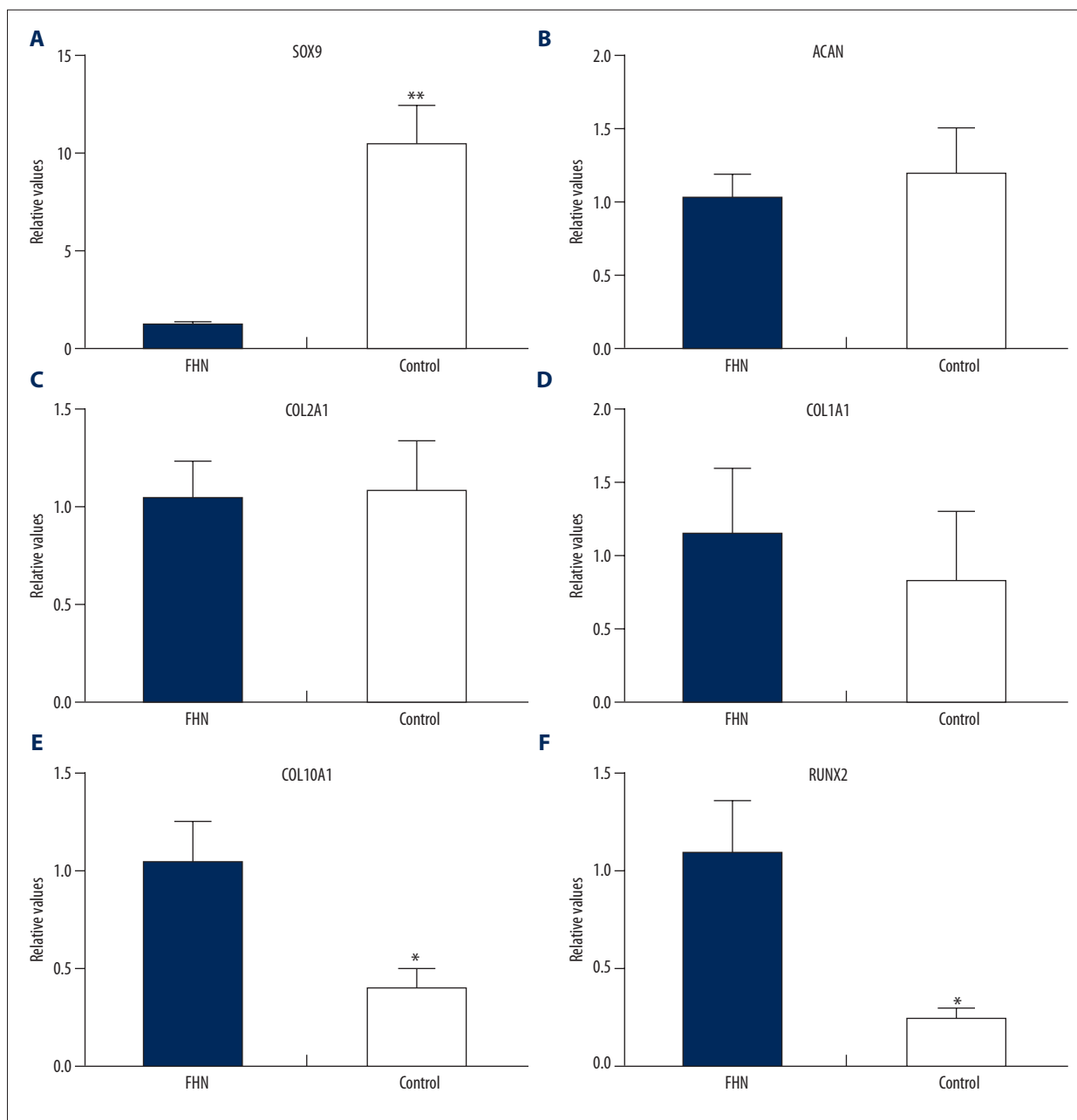


Figure 5. Gene expression detection of femoral head cartilage. (A) Expression of the SOX9 gene in the FHN group was significantly lower than that in the Control group ($P < 0.01$; A). The expressions of ACAN and COL2A1 genes in the FHN group were lower than those in the Control group and the expression of the COL1A1 gene in the FHN group was higher than that in the Control group, but the differences were not statistically significant ($P > 0.05$; B–D). Moreover, the expressions of COL10A1 and RUNX2 genes in the FHN group were significantly higher than that in the Control group ($P < 0.05$; E, F).

Articular cartilage deforms when it is loaded, and the collagen fiber structure carries the stress along the fiber direction to the subchondral bone. It is generally believed that after the collapse of FHN, the structural damage of the subchondral bone causes changes in the stress environment, which leads to degeneration of the articular cartilage [19]. Mankin et al. collected 9 femoral head cartilage samples from patients with

FHN during THA, and found that the femoral head cartilage demonstrated pathological changes, but no significant changes in biochemical and metabolic indexes were detected [34]. Magnussen et al. found that the histological and mechanical changes of post-collapse articular cartilage are highly correlated with gross morphology of the articular cartilage surface in patients with FHN, and further showed the changes in

tensile, compressive, and shear forces caused by FHN [21,22]. However, these studies focused on patients with late-stage FHN after collapse of the femoral head, and few studies have focused on the early stage of FHN prior to collapse. In the present study, we collected samples of femoral head cartilage from patients with early-stage FHN during THA, and evaluated the histological staining and biochemical analysis. Histological staining showed that the number of chondrocytes on the cartilage surface in the FHN group was significantly decreased and the cell arrangement was irregular, and the obvious loss of SO staining and slightly irregular arrangement of collagen fibers appeared on the cartilage surface. Biochemical analysis of the FHN group demonstrated that the water content was significantly increased, the DNA content was significantly decreased, the GAG content was slightly reduced, and the total collagen content was slightly increased, but the difference was not significant, indicating that the FHN group had early cartilage degeneration.

In articular cartilage, proteoglycan-loaded type II collagen fibers form a strong arched structure; proteoglycans inflate this arched structure by absorbing large amounts of water, thereby enabling cartilage tissue to withstand external pressure stress [35]. In the course of FHN, hip articular cartilage is significantly damaged, which increases the instability of the hip and accelerates the development of FHN [21,36]. Therefore, the prevention and early treatment of hip cartilage injury will help slow the progression of FHN. Studies showed that the detection of type II collagen gene expression in patients with necrosis of the femoral head has an important role in the diagnosis and treatment of the disease [34]. Liu et al. explored a variety of gene expressions in articular cartilage in patients with FHN, showing differential expression relative to normal cartilage, such as up-regulation of the type I collagen gene [37]. In the present study, we found that SOX9 gene expression was significantly down-regulated in the FHN group, while COL10A1

and RUNX2 gene expressions were significantly up-regulated. In addition, the expressions of ACAN and COL2A1 in the FHN group were decreased and the expression of COL1A1 gene was increased, but there was no significant difference compared with the Control group. These results suggest that the femoral head cartilage in patients with early THN had early cartilage degeneration.

There are some deficiencies in this study. First of all, the sample size was not large enough, and further research with larger sample sizes is needed. In addition, the femoral head samples of this study were obtained from the weight-bearing area and non-weight-bearing area of the femoral head, as the femoral head necrosis group (FHN group) and the control group (Control group), respectively. However, individual differences may exist among patients, which may have affected the results of the study. Finally, this study did not detect the molecular mechanism of the cartilage matrix degeneration associated with early-stage femoral head necrosis, so its specific mechanisms need to be explored further.

Conclusions

In brief, this study explored the changes in cartilage matrix in early-stage FHN using high-field MRI, histopathological, biochemical, and gene expression analysis. Our results suggest that patients with early-stage FHN have degeneration of the articular cartilage matrix, which provides new ideas for studying the pathogenesis of FHN and selecting optimal treatment strategies.

Conflict of interest

None.

References:

1. Lieberman JR, Berry DJ, Mont MA et al: Osteonecrosis of the hip: management in the 21st century. *Instr Course Lect*, 2002; 52: 337–55
2. Kaushik AP, Das A, Cui Q: Osteonecrosis of the femoral head: An update in year 2012. *World J Orthop*, 2012; 3(5): 49–57
3. Malizos KN, Karantanas AH, Varitimidis SE et al: Osteonecrosis of the femoral head: Etiology, imaging and treatment. *Eur J Radiol*, 2007; 63(1): 16–28
4. Nam KW, Kim YL, Yoo JJ et al: Fate of untreated asymptomatic osteonecrosis of the femoral head. *J Bone Joint Surg Am*, 2008; 90(3): 477–84
5. Issa K, Pivec R, Kapadia BH et al: Osteonecrosis of the femoral head the total hip replacement solution. *Bone Joint J*, 2013; 95(11 Suppl. A): 46–50
6. Pritchett JW: Statin therapy decreases the risk of osteonecrosis in patients receiving steroids. *Clin Orthop Relat Res*, 2001; 386: 173–78
7. Vulpiani MC, Vetrano M, Trischitta D et al: Extracorporeal shock wave therapy in early osteonecrosis of the femoral head: Prospective clinical study with long-term follow-up. *Arch Orthop Trauma Surg*, 2012; 132(4): 499–508
8. Mont MA, Marulanda GA, Seyler TM et al: Core decompression and non-vascularized bone grafting for the treatment of early stage osteonecrosis of the femoral head. *Instr Course Lect*, 2006; 56: 213–20
9. Liu G, Wang J, Yang S et al: Effect of a porous tantalum rod on early and intermediate stages of necrosis of the femoral head. *Biomed Mater*, 2010; 5(6): 065003
10. Yen CY, Tu YK, Ma CH et al: Osteonecrosis of the femoral head: Comparison of clinical results for vascularized iliac and fibula bone grafting. *J Reconstr Microsurg*, 2006; 22(1): 21–24
11. Zhao D, Cui D, Wang B et al: Treatment of early stage osteonecrosis of the femoral head with autologous implantation of bone marrow-derived and cultured mesenchymal stem cells. *Bone*, 2012; 50(1): 325–30
12. Marker DR, Seyler TM, McGrath MS et al: Treatment of early stage osteonecrosis of the femoral head. *J Bone Joint Surg Am*, 2008; 90(Suppl. 4): 175–87
13. Steinberg ME: Diagnostic imaging and the role of stage and lesion size in determining outcome in osteonecrosis of the femoral head. *Techniques in Orthopaedics*, 2001; 16: 6–15
14. Karantanas AH, Drakonaki EE: The role of MR imaging in avascular necrosis of the femoral head. *Semin Musculoskelet Radiol*, 2011; 15(3): 281–300

15. Chang G, Deniz CM, Honig S et al: MRI of the hip at 7T: Feasibility of bone microarchitecture, high-resolution cartilage, and clinical imaging. *J Magn Reson Imaging*, 2014; 39(6): 1384–93
16. Theysohn JM, Kraff O, Orzada S et al: Bilateral hip imaging at 7 Tesla using a multi-channel transmit technology: Initial results presenting anatomical detail in healthy volunteers and pathological changes in patients with avascular necrosis of the femoral head. *Skeletal Radiol*, 2013; 42(11): 1555–63
17. Theysohn JM, Kraff O, Theysohn N et al: Hip imaging of avascular necrosis at 7 Tesla compared with 3 Tesla. *Skeletal Radiol*, 2014; 43(5): 623–32
18. Wei B, Gu Q, Li D et al: Mild degenerative changes of hip cartilage in elderly patients: An available sample representative of early osteoarthritis. *Int J Clin Exp Pathol*, 2014; 7(10): 6493–503
19. Assouline-Dayana Y, Chang C, Greenspan A et al: Pathogenesis and natural history of osteonecrosis. *Semin Arthritis Rheum*, 2002; 32(2): 94–124
20. Ruch DS, Sekiya J, Dickson Schaefer W et al: The role of hip arthroscopy in the evaluation of avascular necrosis. *Orthopedics*, 2001; 24(4): 339–43
21. Magnussen RA, Guilak F, Vail TP: Articular cartilage degeneration in post-collapse osteonecrosis of the femoral head. *J Bone Joint Surg Am*, 2005; 87(6): 1272–77
22. Magnussen RA, Guilak F, Vail TP: Cartilage degeneration in post-collapse cases of osteonecrosis of the human femoral head: Altered mechanical properties in tension, compression, and shear. *J Orthop Res*, 2005; 23(3): 576–83
23. Zalavras CG, Lieberman JR: Osteonecrosis of the femoral head: Evaluation and treatment. *J Am Acad Orthop Surg* 2014; 22(7): 455–64
24. Madry H, Luyten FP, Facchini A: Biological aspects of early osteoarthritis. *Knee Surg Sports Traumatol Arthrosc*, 2012; 20: 407–22
25. Lorenz H, Richter W: Osteoarthritis: Cellular and molecular changes in degenerating cartilage. *Prog Histochem Cytochem*, 2006; 40: 135–63
26. Shindle MK, Foo LF, Kelly BT et al: Magnetic resonance imaging of cartilage in the athlete: current techniques and spectrum of disease. *J Bone Joint Surg Am*, 2006; 88: 27–46
27. Regatte RR, Schweitzer ME: Ultra-high-field MRI of the musculoskeletal system at 7.0 T. *J Magn Reson Imaging*, 2007; 25: 262–69
28. Goebel JC, Bolbos R, Pham M et al: *In vivo* high-resolution MRI (7T) of femoro-tibial cartilage changes in the rat anterior cruciate ligament transection model of osteoarthritis: A cross-sectional study. *Rheumatology*, 2010; 49: 1654–64
29. Mosher TJ, Dardzinski BJ: Cartilage MRI T2 relaxation time mapping: overview and applications. *Semin Musculoskelet Radiol*, 2004; 8: 355–68
30. David-Vaudey E, Ghosh S, Ries M et al: T2 relaxation time measurements in osteoarthritis. *Magn Reson Imaging*, 2004; 22: 673–82
31. Crema MD, Roemer FW, Marra MD et al: Articular cartilage in the knee: Current MR imaging techniques and applications in clinical practice and research. *Radiographics*, 2011; 31: 37–61
32. Apprigh S, Mamisch TC, Welsch GH et al: Quantitative T2 mapping of the patella at 3.0T is sensitive to early cartilage degeneration, but also to loading of the knee. *Eur J Radiol*, 2012; 81: e438–43
33. Apprigh S, Welsch GH, Mamisch TC et al: Detection of degenerative cartilage disease: Comparison of high-resolution morphological MR and quantitative T2 mapping at 3.0 Tesla. *Osteoarthritis Cartilage*, 2010; 18: 1211–17
34. Mankin HJ, Thrasher AZ, Hall D: Biochemical and metabolic characteristics of articular cartilage from osteonecrotic human femoral heads. *J Bone Joint Surg Am*, 1977; 59(6): 724–28
35. Prockop DJ: Type II collagen and avascular necrosis of the femoral head. *N Engl J Med*, 2005; 352(22): 2268–70
36. McCarthy J, Puri L, Barsoum W et al: Articular cartilage changes in avascular necrosis: An arthroscopic evaluation. *Clin Orthop Relat Res*, 2003; 406: 64–70
37. Liu R, Liu Q, Wang K et al: Comparative analysis of gene expression profiles in normal hip human cartilage and cartilage from patients with necrosis of the femoral head. *Arthritis Res Ther*, 2016; 18(1): 98